

3D SIMULATION STUDIES OF TRANSVERSE COHERENT INSTABILITIES IN LONG BUNCHES WITH SPACE CHARGE *

O.Boine-Frankenheim, V. Kornilov, GSI, Planckstr.1, 64291 Darmstadt, Germany

Abstract

3D simulation studies of the transverse impedance budget for long bunches in the FAIR synchrotrons have been started. Important transverse instability driving sources are the thin resistive wall and the kicker impedances. The major concerns are the required low momentum spreads and the additional loss of Landau damping due to the transverse space charge tune shift. The simulation code PATRIC has been extended in order to predict coherent instability thresholds with space charge and for broadband impedance sources. Simulation scans were performed to analyze the improvement of transverse stability in long bunches relative to a coasting beam.

INTRODUCTION

The FAIR synchrotrons, SIS 18 and the planned SIS 100, will be operated with medium energy, intense heavy ion beams of low momentum spread. The range of bunch lengths and bunch profiles during a typical cycle covers dc beams, long dc-like bunches in barrier buckets, long bunches in single and in dual rf waves [1]. Before extraction the bunches are converted into a single, short (50 ns) bunch. The required accumulation times in SIS 100 are of the order of 1 s. Because of the high intensities together with low momentum spreads transverse instabilities driven by the thin resistive wall [2] or kickers impedances [3, 4, 5] are of concern. In addition the bunches will experience relatively large transverse space charge tune shifts, compared to the effective tune spreads for Landau damping. Space charge itself will not drive coherent instabilities, but is can greatly modify the stability boundaries (see e.g. [6]). The space charge induced 'loss of Landau damping' in coasting beams has been analyzed in Ref. [7]. In bunched beams the variation of the incoherent space charge tune shift and of the coherent tunes shifts along the bunch result in additional effective tune spreads. Simulation studies performed for the SNS accumulator ring [8] indicate that the stability limit is increased in long bunches relative to the equivalent coasting beam. Here we will report first results from a systematic simulation study of stability limits with space charge in long bunches using the particle tracking code PATRIC [9].

TRANSVERSE IMPEDANCE SPECTRUM

The thin resistive beam pipe together with the injection/extraction kicker modules represent important

impedance contributions in SIS 18 and SIS 100. The beam pipe impedance affects the coherent betatron sidebands between ≈ 50 kHz and 1 MHz, depending on the machine tune. In order to reduce eddy current effects, the stainless steel beam pipe in the SIS 18 magnets is only 0.3 mm thick. The skin depth is 1 mm at the injection energy of 11.4 MeV/u. For the stainless steel beam pipe in the planned SIS 100 magnets, a wall thickness of a few 0.1 mm will be required. In addition to the large impedance contribution of a thin beam pipe at low frequencies also the shielding effectiveness of the pipe is of importance [2]. The impedance of the ferrite-loaded kickers can be divided into two parts [5]. Below frequencies ≈ 50 MHz the horizontal impedance is dominated by the external circuit. Above ≈ 200 MHz the Ferrite contribution dominates. For coasting beams and for long bunches we are concerned about transverse impedances below ≈ 50 MHz. Fig. 1 shows the calculated transverse impedances (real parts) of the resistive wall and of the kickers in SIS 18 for 200 MeV/u beam energy. In the beam dynamics simulations we will use a transverse oscillator model with $Q_r = 2$ and resonance frequency $f_r \approx 8$ MHz as a rough approximation of the kicker impedance. The resulting curve is shown in Fig. 1. Because the beams in the FAIR synchrotrons typically fill a large fraction of the pipe, the dominant imaginary impedance contribution is expected to arise from the image currents. The corresponding space charge impedance is

$$Z_{\perp}^{sc} = -i \frac{Z_0 R}{\beta_0^2 \gamma_0^2 b^2} \quad (1)$$

with the ring radius R , the beam pipe radius b , the relativistic factors β_0 and γ_0 .

In Fig. 1 also the threshold impedance for coasting beam transverse instabilities is shown. This threshold is calculated from the circle criterium (see e.g.[6])

$$|\Delta\Omega_c - \omega_0 \Delta Q| \lesssim FS\delta_{rms} \quad (2)$$

with the revolution frequency ω_0 , the space charge tune shift ΔQ , the effective chromaticity

$$S = \omega_0 (\xi - (n \pm Q_0)\eta_0) \quad (3)$$

the form factor F , the harmonic number n , the rms momentum spread δ_{rms} and the coherent frequency shift

$$\Delta\Omega_c = -\frac{i}{8\pi^2} \frac{q^2 N}{m\gamma_0 c Q_0} Z_{\perp} \quad (4)$$

with the bare tune Q_0 , particle number N , charge q and mass m . In Fig. 1 one can see that the 'loss of Landau damping' due to the space charge tune shift is effective below ≈ 10 MHz. Here the impedance budget for a coasting

* Work supported by EU design study (contract 515873 - DIRACsecondary-Beams)

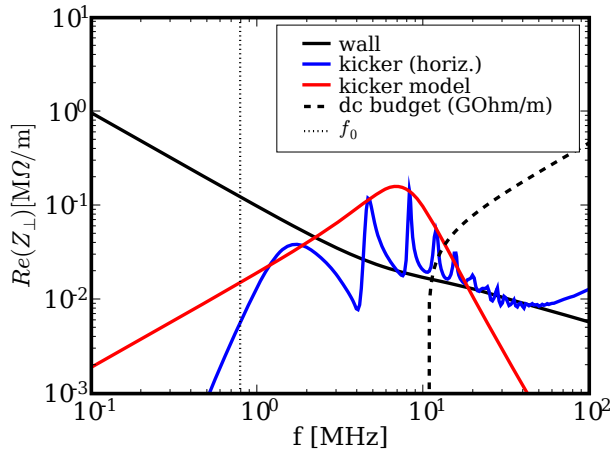


Figure 1: Calculated transverse impedance spectrum for SIS 18. Shown are the resistive wall impedance and the horizontal kicker impedance (real parts). The dashed curve represents the 'impedance budget' for a coasting beam.

beam would be essentially zero, provided that no additional Landau damping mechanisms are effective. At higher frequencies Landau damping due to finite momentum spread leads to a sufficient stabilization of coasting beams.

IMPLEMENTATION OF IMPEDANCE KICKS IN PATRIC

PATRIC [9] is a 3D tracking code developed at GSI for simulation studies of coherent instabilities with self-consistent space charge in ring accelerators. In this section we will describe the implementation of impedance kicks in PATRIC, which is similar to the scheme presented in Ref. [10]. The 'dipole moment times current' at a fixed ring position s is $\psi(t)$. The resulting horizontal kick per turn (see e.g. [10]) is

$$\Delta x'_{imp} = \frac{\int F_{\perp} ds}{\beta_0^2 E_0} = \quad (5)$$

$$\text{Re} \left(\frac{iq}{\beta_0 E_0} \sum_j \psi_j Z_{\perp}(\Omega_j) \exp(i\Omega_j t) \right)$$

with the frequency spectrum $\psi(\Omega_j)$ at the coherent dipole oscillation frequencies

$$\Omega_j \approx (n \pm Q_0)\omega_0 \quad (6)$$

The horizontal dipole moment along the longitudinal particle position z is defined as

$$\psi(z, t) = \beta_0 c \int x \rho(x, y, z, t) dx dy \quad (7)$$

and the Fourier spectrum is (ring circumference L)

$$\psi_n^{\pm}(t) = \exp(\mp i Q_0 \omega_0 t) \int_0^L \psi(z, t) \exp(-inz/R) dz \quad (8)$$

The amplitude $\psi_n(t)$ varies slowly with time. For lumped impedances the resulting kick is applied every Δs

$$\Delta x'_{imp}(z, t) = \frac{\Delta s}{L} \frac{q}{\beta_0 E_0} \times \quad (9)$$

$$\text{Re} \left(i \exp(\pm i Q_0 \omega_0 t) \sum_n \psi_n^{\pm}(t) Z_{\perp} [(n \pm Q_0)\omega_0] \exp(inz/R) \right)$$

For a localized impedance source we set $\Delta s = L$ and the kick is applied every turn.

APPLICATION TO LONG BUNCHES IN SIS 18

Our aim is to compare the transverse stability boundaries for long bunches in rf buckets and in barrier buckets with the equivalent coasting beam. Therefore we perform parameter scans by varying the imaginary space charge impedance $Z_I = Z_{\perp}^{sc}$ and the maximum real value of the transverse oscillator impedance $Z_R = Z_{\perp}^{\max}$ approximating the kicker. The beam parameters are chosen according to the expected values for U^{28+} beams in SIS 18 at 200 MeV/u, which is the injection energy for SIS 100. The resonant frequency of the oscillator impedance at the harmonic number $n = f_{res}/f_0 \approx 10$. The coasting beam space charge tune shift is $\Delta Q = -0.05$. Instead of the self-consistent space charge solver we use a linear space charge force which is proportional to the local line density and which moves with the local offset. Fig. 2 shows the obtained maximum beam offset amplitude for different (Z_R, Z_I) and for a coasting beam with an elliptic momentum distribution. One can see that the beam offset remains at the initial noise level for impedances inside the stability boundary obtained from the dispersion relation. Differences between the analytic stability boundary and the simulation results for low Z_R can e.g. be addressed to the finite simulation time. Fig. 2 is also a code validation example. The expected kicker and space charge impedances in SIS 18 are indicated in Fig. 2 as a red dot.

In the case of a beam with a small gap (covering 20% of the ring circumference) provided by barrier rf pulses we obtain a stability boundary that is very close to the one for the equivalent coasting beam. Fig. 3 shows a snap shot of the instability evolution in the rf barrier bucket. Outside the coasting beam stability boundary and for small Z_R we observe a saturation of the instability at moderate amplitudes (inside the aperture). The bunch remains in a turbulent state.

For a parabolic bunch profile the situation is different. In Fig. 4 we observe a larger threshold impedance Z_R with increasing image current impedance $|Z_I|$. This behavior can be explained in terms of the coherent frequency shift variation along the bunch. The maximum coherent frequency shift $\Delta\Omega_c^{sc}$ at the bunch center due to the image currents is given through Eq. (4) with $Z_{\perp} = Z_{\perp}^{sc}$. The resulting coherent frequency spread is $\delta\Omega = |\Delta\Omega_c^{sc}|$. For the $m = 0$ mode (rigid-bunch oscillation) this frequency

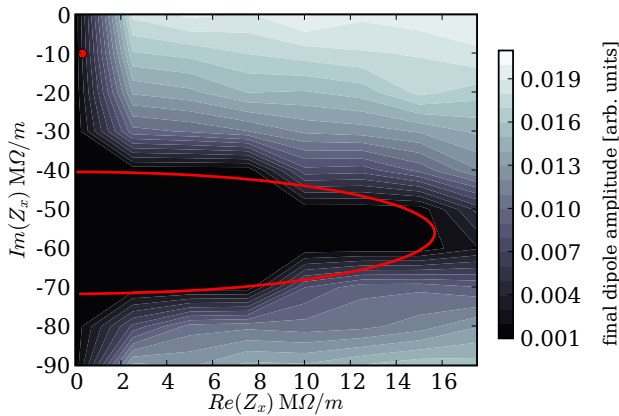


Figure 2: Maximum beam offset amplitude for a coasting beam as a function of (Z_R, Z_I) . The curve represents the stability boundary obtained analytically for an elliptic momentum spread distribution.

spread can be directly associated with the damping rate. For $m > 0$ the effective spread per wave length will be smaller. A possible scaling law for the damping rate is

$$\tau_c^{-1} \propto \frac{|\Delta\Omega_c^{sc}|}{m} \quad (10)$$

If we simply equate this damping rate with the growth rate from Eq. (4) with $Z_{\perp} = Z_R$ we obtain the following threshold law

$$Z_R \lesssim \frac{|Z_{\perp}^{sc}|}{m} \quad (11)$$

which approximates very well the simulation results, if we set $m \approx 25$ (see Fig. 4). However, the observed mode number is close to $m \approx 8$. More studies are needed to understand this damping mechanism for modes $m > 0$ and also for different bunch profiles (e.g. in barrier buckets). It is important to point out, that the linear space charge tune shift along the bunch does not cause damping.

CONCLUSIONS

The stability of transverse coherent oscillations in long bunches with space charge under conditions relevant for the FAIR synchrotrons has been studied. We compare the instability thresholds obtained from simulation scans for bunched beams and for the equivalent coasting beams. We find that the coherent frequency shift along the bunch, that results from image currents, can lead to a stabilization. The equivalent coasting beam would be unstable due to the space charge induced loss of Landau damping. A more detailed understanding of the responsible damping mechanism still needs to be developed. The coherent frequency shift in barrier buckets is mostly constant along the bunch and therefore the stability properties are very close to coasting beams.

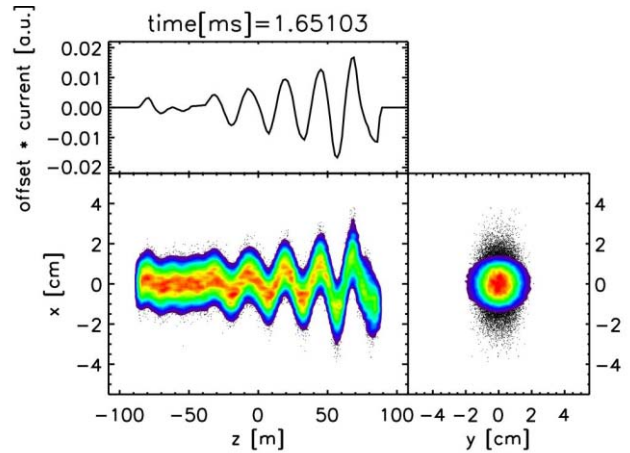


Figure 3: Snap shot of the instability evolution in a barrier rf bucket. Shown are contour plots of the densities in (x, z) and (x, y) phase space together with the dipole moment along the z axis.

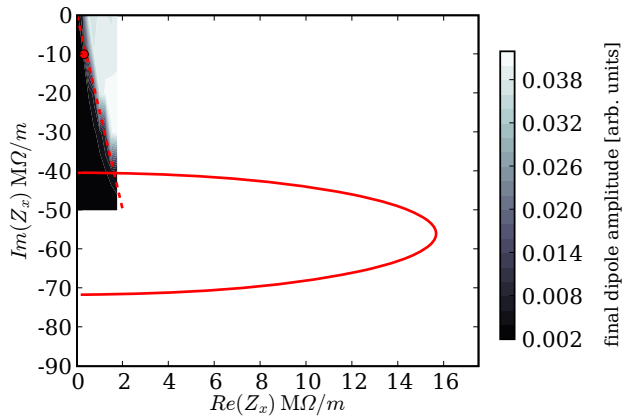


Figure 4: Maximum beam offset amplitude in a bunch as a function of (Z_R, Z_I) . The curve represents the stability boundary obtained analytically for a coasting beam and an elliptic momentum spread distribution. The dashed line represents Eq. (11) with $m = 25$. The simulation scan has been concentrated on a thin strip along the Z_I axis in order to resolve the stability threshold.

REFERENCES

- [1] P. Spiller, Proc. of PAC 2005, p.294
- [2] A. Al-khateeb, et al., Phys. Rev. ST-AB **10**, 064401 (2007)
- [3] U. Blell, Proc. of PAC 1997, p. 1727
- [4] B. Doliwa, et al., Proc. of PAC 2005, p. 1822
- [5] B. Doliwa, Th. Weiland, Proc. of ICAP 2006, p. 277
- [6] O. Boine-Frankenheim, Proc. of EPAC 2006, p. 1886
- [7] K.Y.Ng, AIP Conf. Proc. **773**, 365 (2005)
- [8] A. Fedotov, J. Wei, V. Danilov, Proc. of PAC 2003, p. 3032
- [9] O. Boine-F., V. Kornilov, Proc. of ICAP 2006, p. 267
- [10] V. Danilov et al., Proc. of PAC 2001, p. 1752